Supplementary Information for

Interface engineering of $Li_{6.75}La_3Zr_{1.75}Ta_{0.25}O_{12}$ via in-situ built $LiI/ZnLi_x$ mixed buffer layer for solid-state lithium metal batteries

Lei Zhai [a], Jinhuan Wang [a], Xiaoyu Zhang [a], Xunzhu Zhou [b], Fuyi Jiang [a], Lin Li [b,*], Jianchao Sun [a,*]

a. School of Environment and Material Engineering, Yantai University, Yantai 264005, Shandong, China. E-mail: jianchaoabc@163.com.

b. Institute for Carbon Neutralization, College of Chemistry and Materials Engineering, Wenzhou University, Wenzhou, Zhejiang 325035, China. linli@wzu.edu.cn.

Methods and experimental

Preparation of LLZTO

LLZTO was prepared by solid phase reaction method using $LiOH·H_2O$, La_2O_3, ZrO_2 and Ta_2O_5 as raw materials. An excess of 10% $LiOH·H_2O$ was added to the raw materials to compensate for the loss of lithium in the sintering process. The mixture was calcined at 900 °C for 6 h, and then ground to obtain LLZTO precursor powder. The LLZTO precursor powder was pressed into plate-like discs, sintered at 1100 °C for 2 h, and slowly cooled at 3 °C min^{-1} to obtain dense LLZTO pellets with diameter of 15.0 mm and thickness of 1.0 mm. Finally, the LLZTO pellets were polished with sandpaper to achieve a mirror-like effect. The polished pellets are stored in a glove box filled with argon gas.

Preparation of ZnI_2@LLZTO

A series of ZnI_2 solutions with different concentrations were prepared with anhydrous ethanol as solvent (0.1, 0.3, 0.5, 1.0, 1.5 mol L^{-1}). ZnI_2@LLZTO pellets were prepared by placing the bare LLZTO pellets in ZnI_2 solution for 10 seconds. Then, the obtained ZnI_2@LLZTO pellets were dried under vacuum at 60 °C for 1 h. According to the different concentration of ZnI_2 solution, the prepared samples were named as ZnI_2@LLZTO-0.1, ZnI_2@LLZTO-0.3, ZnI_2@LLZTO-0.5, ZnI_2@LLZTO-1.0, ZnI_2@LLZTO-1.5, respectively. In particular, ZnI_2@LLZTO-0.5 is replaced by ZnI_2@LLZTO in the following description.

Preparation of LiI/$ZnLi_x$@LLZTO

First, heat ZnI_2@LLZTO on a hot plate. When the temperature rises to 180 °C, place the Li metal sheet on ZnI_2@LLZTO and continue heating to 220 °C (reserve for 10 seconds). Then stop heating and wait for cooling. All operations are performed in the glove box.

Materials Characterizations

Scanning electron microscope (SEM) was used to obtain the morphology of prepared materials (JSM-7610F). X-ray diffraction (XRD) patterns were performed at a Rigaku D/MAX 2500/PC diffractometer with Cu-Kα radiation. X-ray photoelectron spectroscopy (XPS) measurements were conducted to analyze composite components (ESCALAB 250Xi). Electrochemical impedance spectroscopy (EIS) was collected in the range of 10^{-2} ~ 10^{6} Hz.

Finite element analysis (FEA) simulation

A 2D model was established to compare the proportional schematics of local current density and electric field distribution. The local current density is solved according to the Butler-Volmer equation.

Electrochemical Characterizations

To assemble Li/LLZTO/Li or Li/ZnI_2@LLZTO/Li symmetrical cells, Li metal electrodes are coated on either side of solid-state electrolyte. $LiFePO_4$ cathode was prepared by a mixture of 10 wt% polyvinylidene fluoride, 20 wt% carbon black and 70 wt% $LiFePO_4$. The active material loading of cathode was controlled to be about 3.0 mg cm^{-2}. To eliminate external distractions in evaluating the Li/LLZTO interface, 10 μL liquid organic electrolyte (1 M $LiPF_6$ in EC/DEC) was added between the LLZTO

pellet and cathode to weaken the interfacial resistance. In the symmetric cells, the buffer layer is on both sides of LLZTO. In the full cell, the buffer layer is only on one side of LLZTO. The full cell test was performed at 2.5-4.1 V with different current rates (1 C= 170 mA g^{-1}). The operating temperature for every performance test was performed at room temperature, unless otherwise specified.

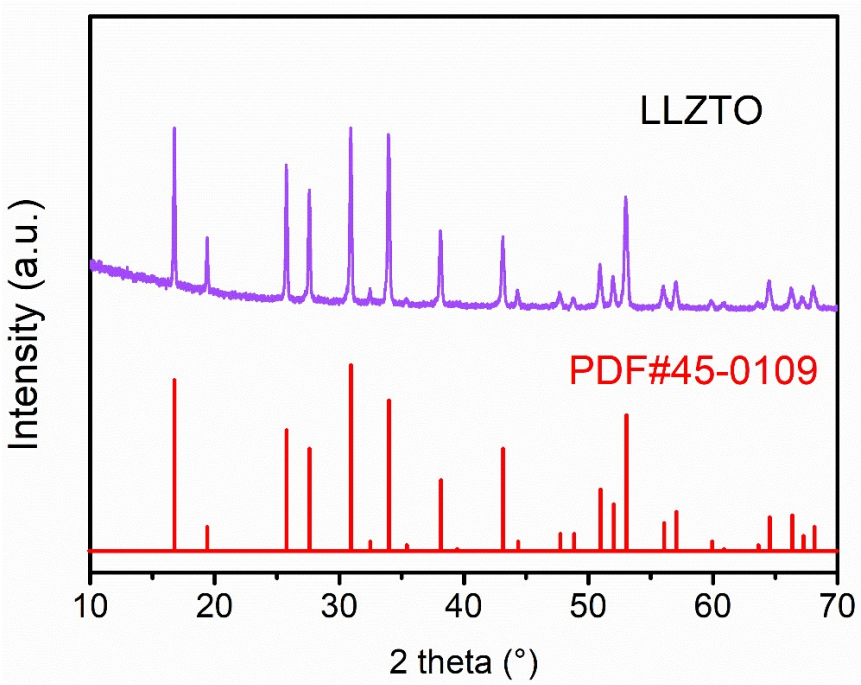

Figure S1. XRD pattern of LLZTO powder.

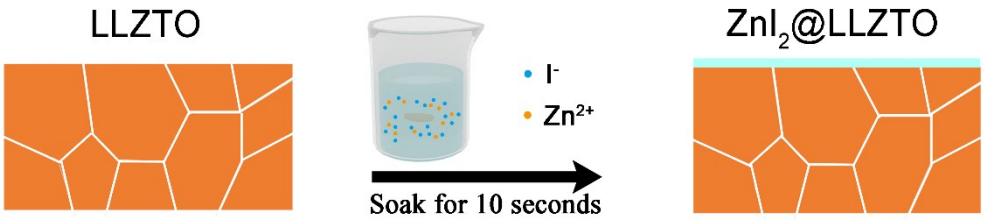

Figure S2. Schematic illustration of the preparation of ZnI_2@LLZTO.

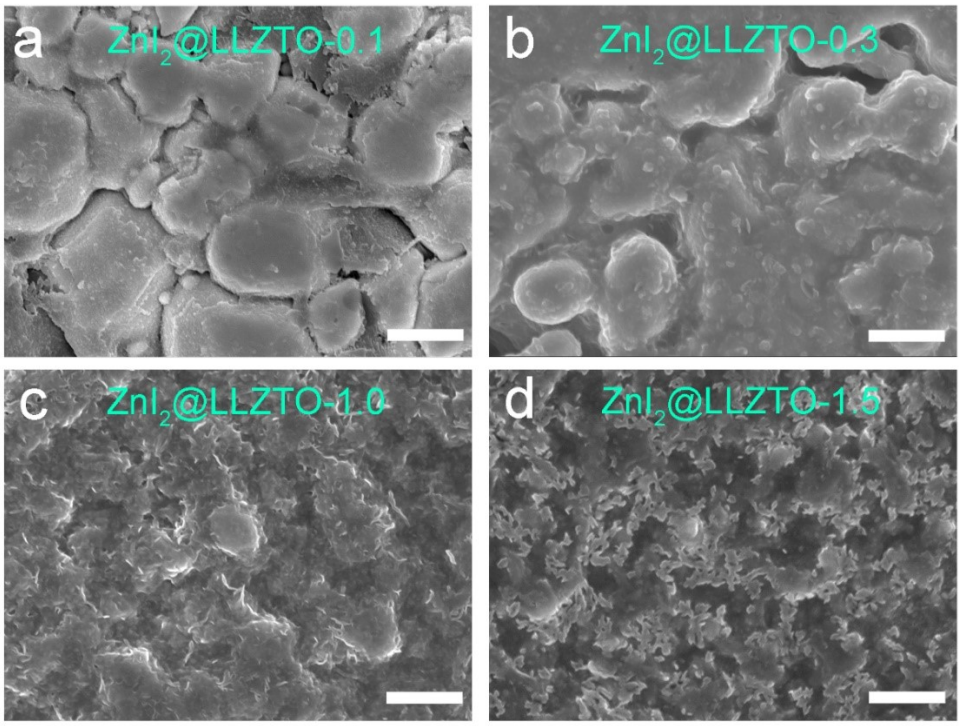

Figure S3. SEM images of **a** ZnI_2@LLZTO-0.1, **b** ZnI_2@LLZTO-0.3, **c** ZnI_2@LLZTO-1.0, **d** ZnI_2@LLZTO-1.5. Scale bar, 1 μm.

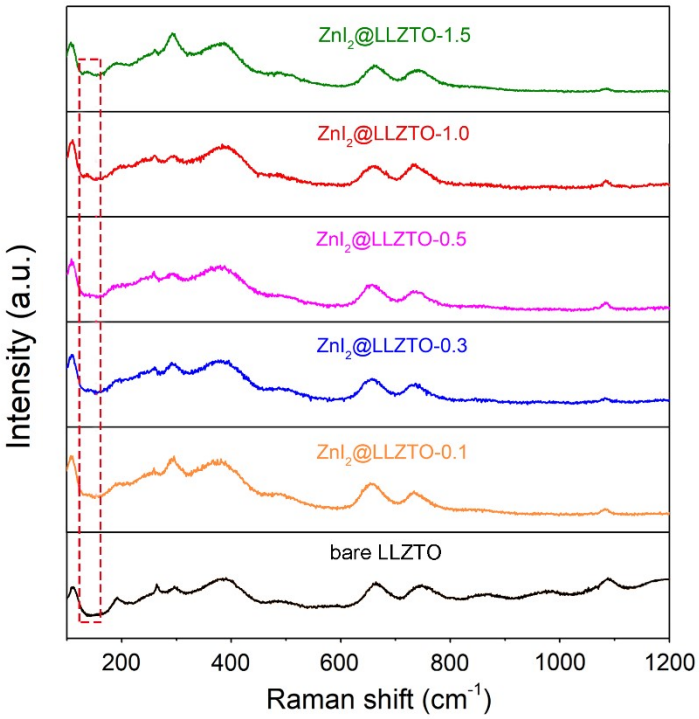

Figure S4. Raman spectra of LLZTO treated with different concentrations of ZnI_2 solution.

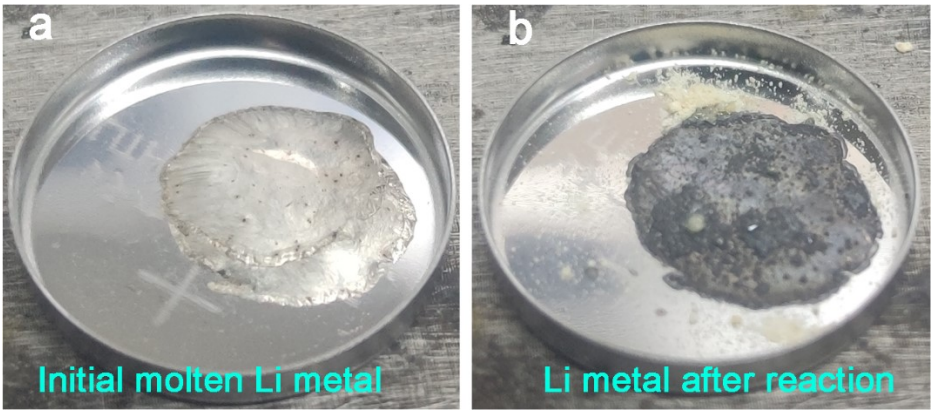

Figure S5. Photographs of Li reacting with ZnI_2: **a** before and **b** after the reaction.

The color changes from silver to black.

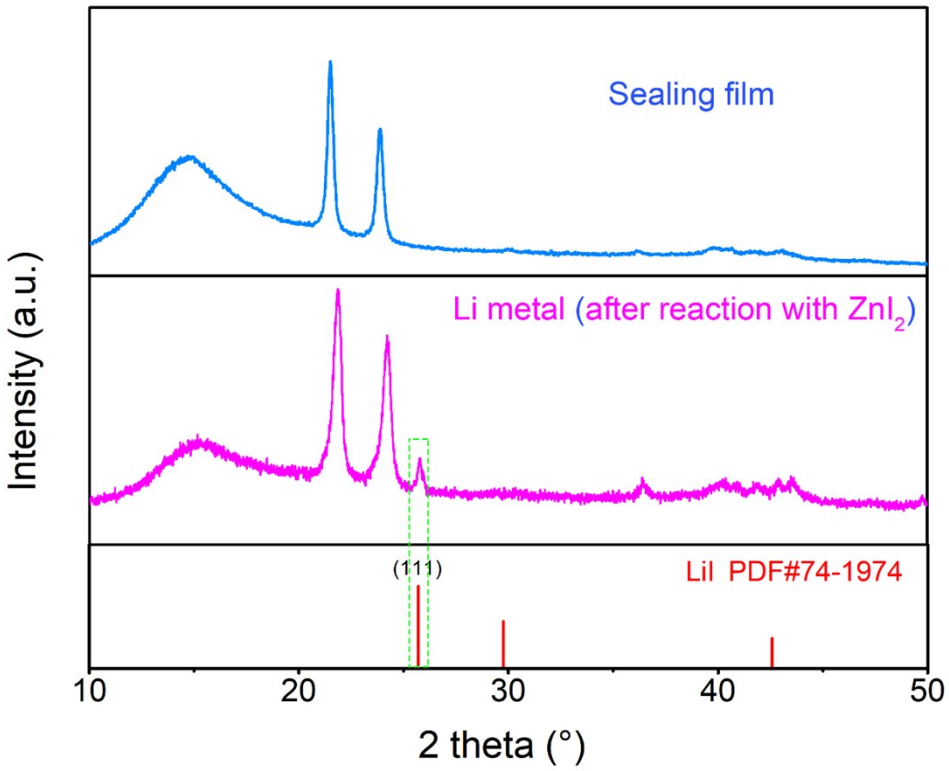

Figure S6. XRD pattern of Li metal after reaction.

The above experiments show that the reaction between ZnI_2 and Li metal is: (2+x) Li + $ZnI_2 \rightarrow$ 2 LiI + $ZnLi_x$.

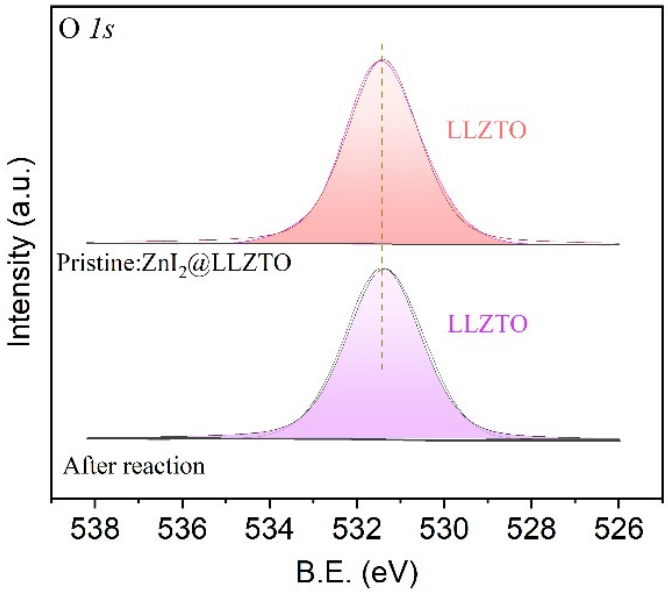

Figure S7. High-resolution O 1*s* XPS analysis of ZnI_2@LLZTO pellet surface before and after reaction.

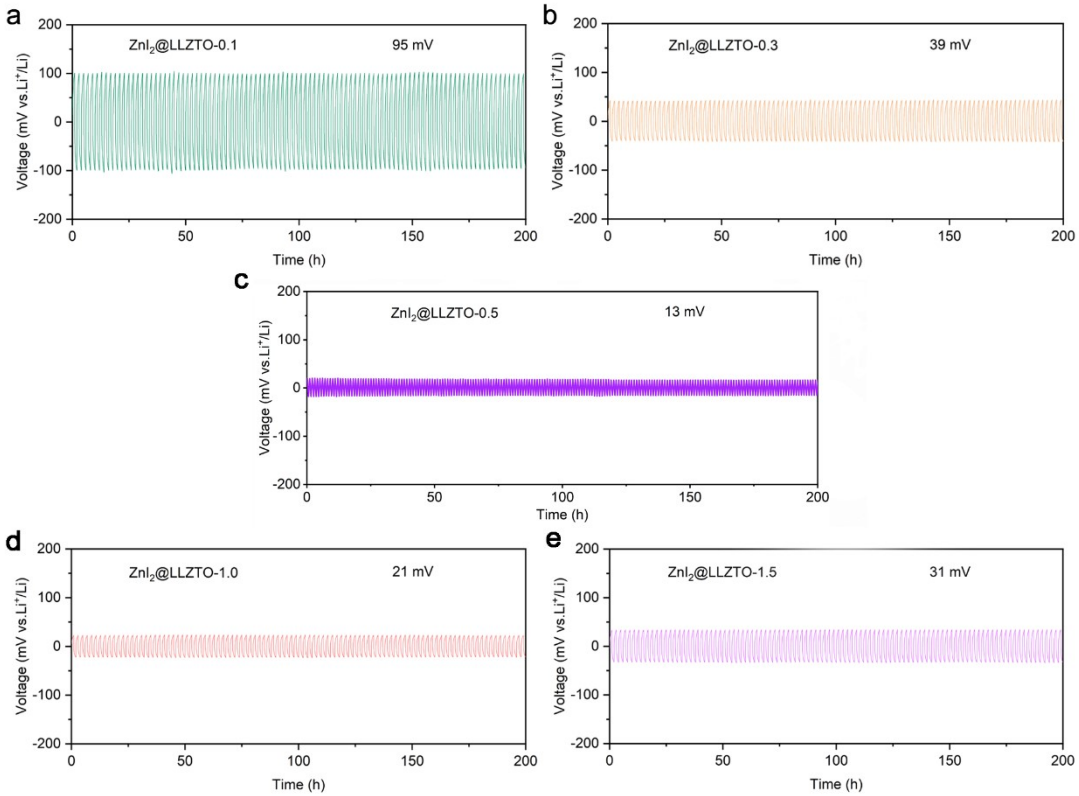

Figure S8. Charge-discharge voltage profiles of Li/ZnI_2@LLZTO/Li cells with different concentrations of ZnI_2 at 0.1 mA cm^{-2} with 0.1 mAh cm^{-2}.

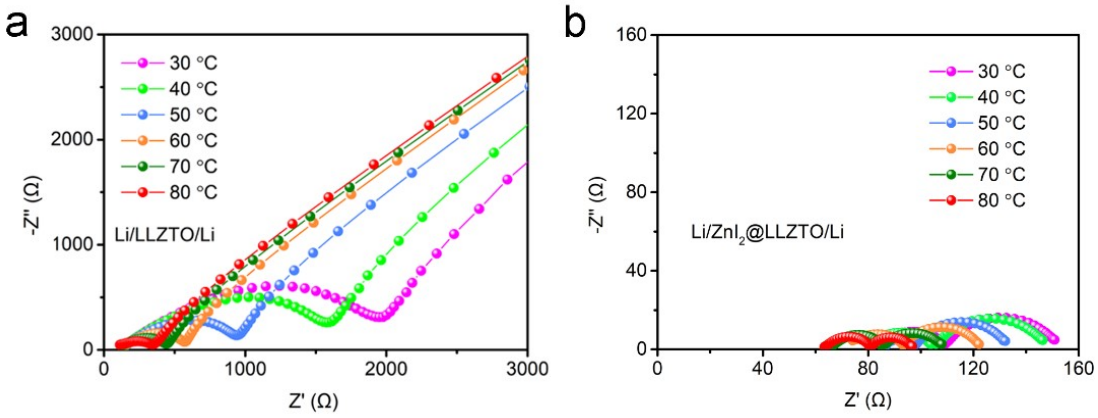

Figure S9. Interface resistance of Li/LLZTO/Li and Li/ZnI_2@LLZTO/Li cells at different temperatures.

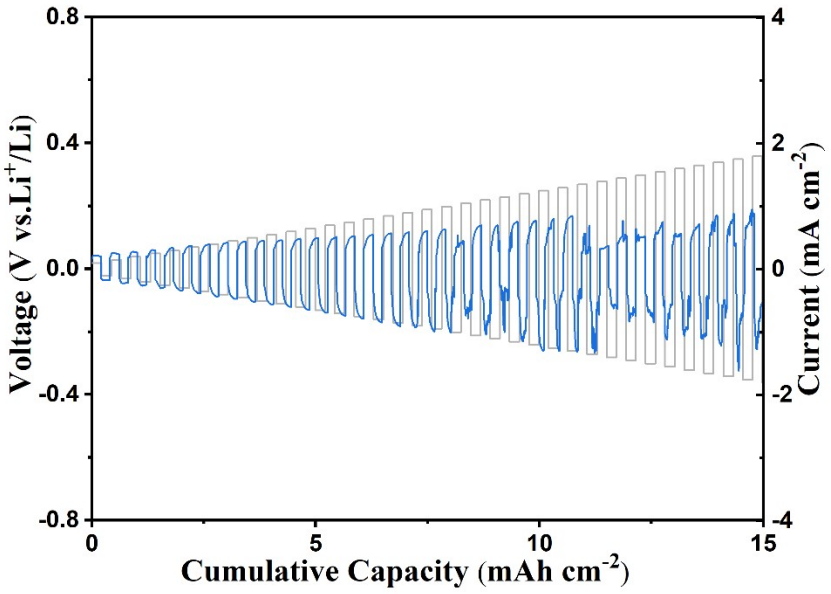

Figure S10. Critical current density test of Li/SSE/Li cells with 1.5 mol/L ZnI_2.

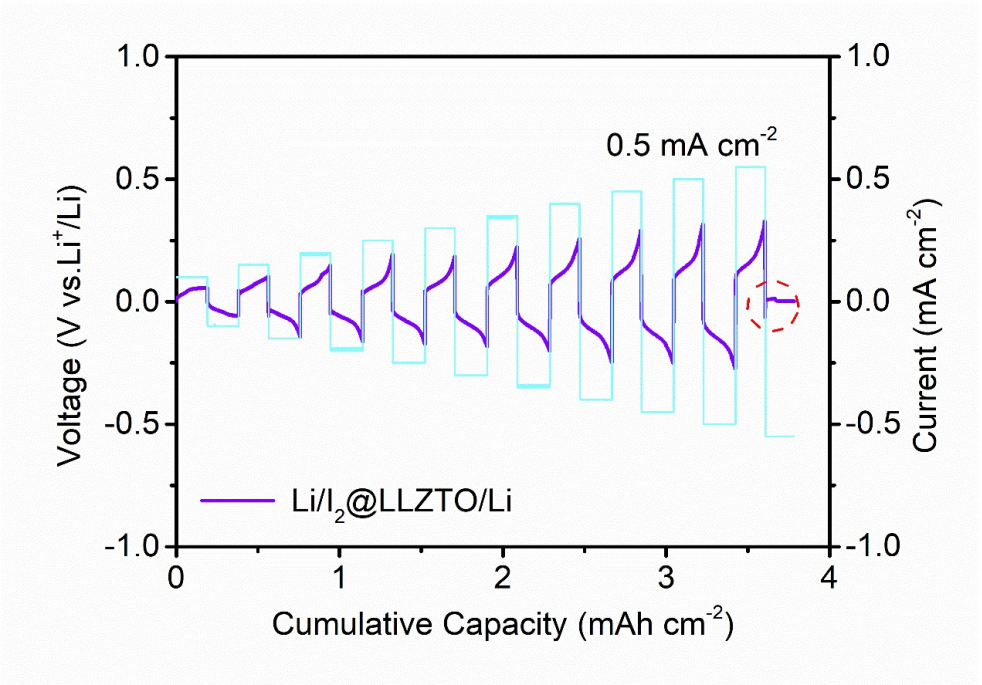

Figure S11. Critical current density test of Li/SSE/Li cells with I_2 buffer layer.

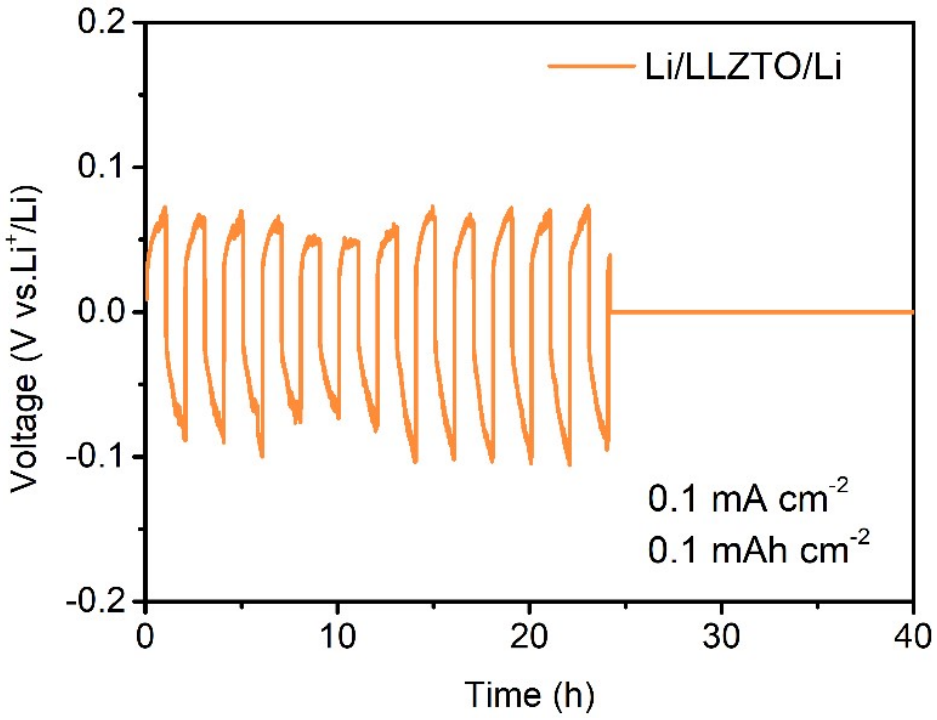

Figure S12. Long-term plating/stripping profiles of Li/LLZTO/Li cells at 0.1 mA cm^{-2} and 0.1 mAh cm^{-2}.

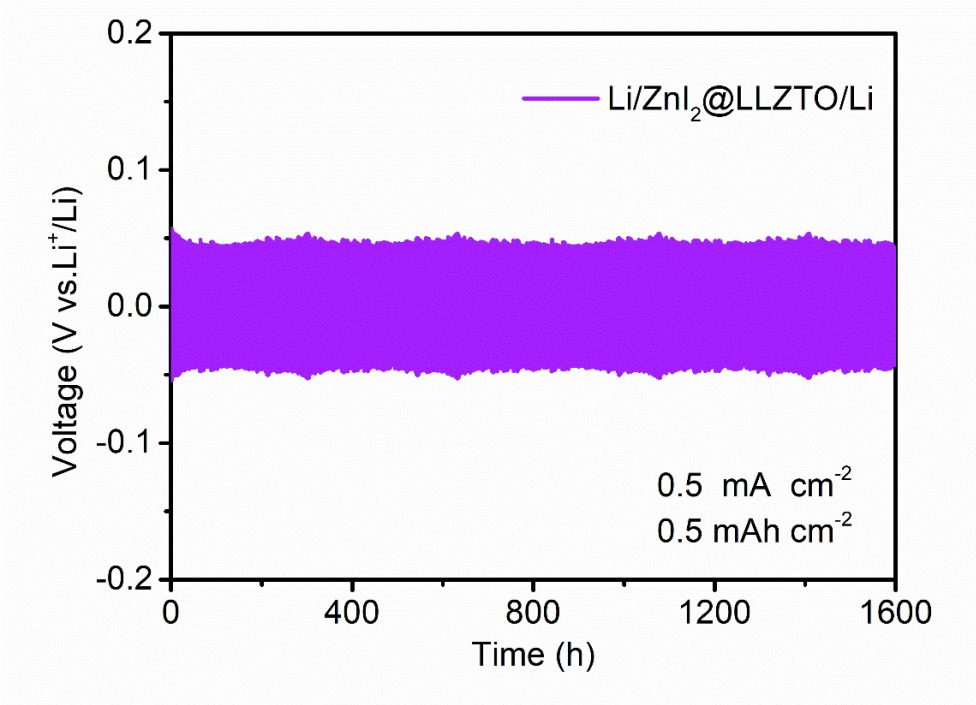

Figure S13. Charge-discharge voltage profiles of Li/ZnI_2@LLZTO/Li cells at 0.5 mA cm^{-2} and 0.5 mAh cm^{-2}.

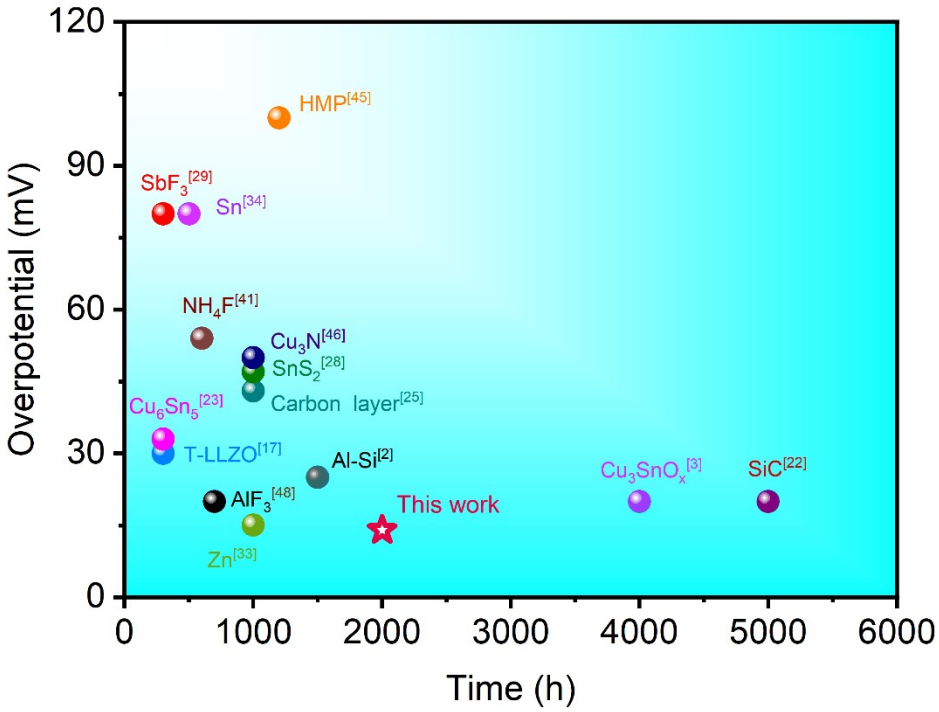

Figure S14. The overpotential comparison of symmetric cells with LLZTO modified in different ways at 0.1 mA cm^{-2}.

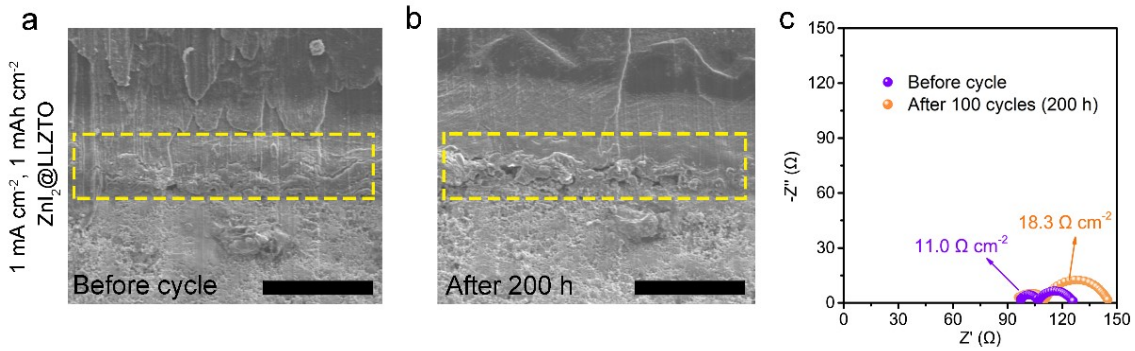

Figure S15. The cross-sectional SEM images and Nyquist plots of Li/ZnI_2@LLZTO/Li symmetrical cells before and after cycles at 1 mA cm^{-2} and 1 mAh cm^{-2}.

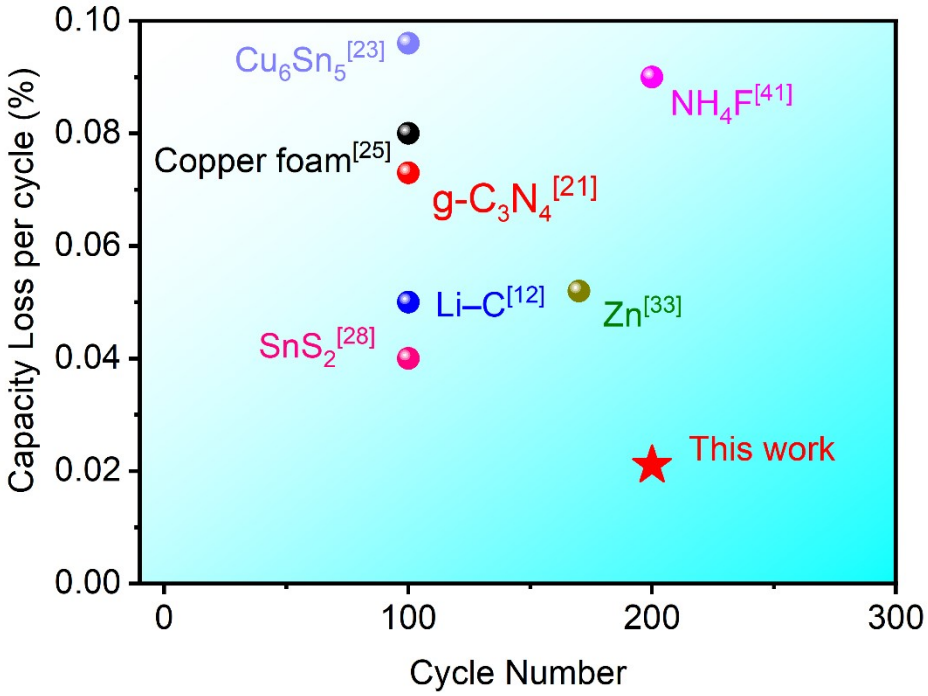

Figure S16. The comparison of capacity loss per cycle for solid-state batteries at 0.5 C.

Table S1. Comparison of battery performance with different treatment methods.

Reference	Improvement measure	Current density (mA/cm^2)	Time (h)	CCD (mA/cm^2)
This work	ZnI_2	0.1	2000	2.3
		0.5	1600	
		1.0	800	
28	SnS_2	0.1	1000	0.5
		0.2	1000	
21	g-C_3N_4	0.3	300	1.5
12	Li-C	0.3	250	1.5
41	NH_4F	0.3	600	1.4
		0.4	250	
		0.5	250	
46	Cu_3N	0.1	1000	1.2
43	SnO_2	0.2	650	1.15
2	Al-Si	0.1	1500	1.2
		1.0	800	
18	Sb	0.2	350	0.64
33	Zn	0.1	1000	2.0
		0.5	300	
45	HMP	0.1	1200	1.91
		0.3	400	
34	Sn	0.5	500	-
25	Copper foam	0.3	600	-
23	Cu_6Sn_5	0.1	300	-
		0.25	300	
29	SbF_3	0.2	320	0.6
17	T-LLZO	0.15	300	-
3	Cu_3SnO_x	0.2	4000	3.0
		4.0	1600	

22	SiC	3.5	1000	4.6
48	AlF_3	0.5	670	3.0

Reference

2. L. Zhai, K. Yang, F. Jiang, W. Liu, Z. Yan, J. Sun, *J. Energy Chem.*, 2023, **79**, 357-364.

12. J. Duan, W. Wu, A. M. Nolan, T. Wang, J. Wen, C. Hu, Y. Mo, W. Luo, Y. Huang, *Adv. Mater.*, 2019, **31**, 1807243.

17. J. Gao, J. Zhu, X. Li, J. Li, X. Guo, H. Li, W. Zhou, *Adv. Funct. Mater.*, 2021, **31**, 2001918.

18. R. Dubey, J. Sastre, C. Cancellieri, F. Okur, A. Forster, L. Pompizii, A. Priebe, Y. Romanyuk, L. Jeurgens, M. Kovalenko, K. Kravchyk, *Adv. Energy Mater.*, 2021, **11**, 2102086.

21. Y. Huang, B. Chen, J. Duan, F. Yang, T. Wang, Z. Wang, W. Yang, C. Hu, W. Luo, Y. Huang, *Angew. Chem. Int. Ed.*, 2020, **59**, 3699-3704.

23. W. Feng, X. Dong, Z. Lai, X. Zhang, Y. Wang, C. Wang, J. Luo, Y. Xia, *ACS Energy Lett.*, 2019, **4**, 1725-1731.

25. J. Duan, L. Huang, T. Wang, Y. Huang, H. Fu, W. Wu, W. Luo, Y. Huang, *Adv. Funct. Mater.*, 2020, **30**, 1908701.

28. B. Zhao, W. Ma, B. Li, X. Hu, S. Lu, X. Liu, Y. Jiang, J. Zhang, *Nano Energy*, 2022, **91**, 106643.

29. A. Wang, J. Li, M. Yi, Y. Xie, S. Chang, H. Shi, L. Zhang, M. Bai, Y. Zhou, Y. Lai, Z. Zhang, *Energy Storage Mater.*, 2022, **49**, 246-254.

33. Z. Wan, K. Shi, Y. Huang, L. Yang, Q. Yun, L. Chen, F. Ren, F. Kang, Y. He, *J. Power Sources*, 2021, **505**, 230062.

34. M. He, Z. Cui, C. Chen, Y. Li, X. Guo, *J. Mater. Chem. A*, 2018, **6**, 11463-11470.

41. H. Duan, W. Chen, M. Fan, W. Wang, L. Yu, S. Tan, X. Chen, Q. Zhang, S. Xin, L. Wan, Y. Guo, *Angew. Chem. Int. Ed.*, 2020, **59**, 12069-12075.

43. Y. Chen, M. He, N. Zhao, J. Fu, H. Huo, T. Zhang, Y. Li, F. Xu, X. Guo, *J. Power Sources*, 2019, **420**, 15-21.

45. Z. Qin, Y. Xie, X. Meng, D. Qian, C. Shan, D. Mao, G. He, Z. Zheng, L. Wan, Y. Huang, *Chem. Eng. J.*, 2022, **447**, 137538.

46. Q. Ma, X. Zhang, A. Wang, Y. Xia, X. Liu, J. Luo, *Adv. Funct. Mater.*, 2020, **30**, 2002824.